

# Spin and valley transport in the ferromagnetic MoS<sub>2</sub> junctions subjected by the gate voltage

P. Ye<sup>1</sup>, R.Y. Yuan<sup>1</sup>, Y. Y. Xia<sup>1</sup>, X. Zhao<sup>2</sup>

<sup>1</sup>Center for Theoretical Physics, Department of Physics, Capital Normal University, Beijing 100048, China.

<sup>2</sup>Department of Physics and State Key Laboratory of Low-Dimensional Quantum Physics, Tsinghua University, Beijing 100084, China

Electronic address: yuanry@cnu.edu.cn

**Abstract.** In this paper, we have studied valley and spin-polarized transport with different gate voltage in ferromagnetic MoS<sub>2</sub> junctions. The results show that, the valley and spin transport through the junctions has a large oscillation. In particular, a fully spin polarized current can be put out by effectively tuning the gate voltage  $U$ . Moreover, with increasing of  $U$ , the scope of the valley and spin polarization can be greatly expanded. These findings indicate the structure is a considerable candidate for the spintronics or valleytronics device.

## 1. Introduction

The monolayer (ML) MoS<sub>2</sub>, a typical two-dimensional (2D) material, have attracted growing attention. The ML MoS<sub>2</sub> has a relatively large direct energy gap compared to graphene[2], possessing high carrier mobility, large thermal stability and good compatibility with standard semiconductor manufacturing[3]. These remarkable physical properties make ML MoS<sub>2</sub> as potential applications in next-generation nanoelectronic devices. Moreover, ML MoS<sub>2</sub> has strong spin-orbit coupling (SOC) absent in graphene[4,11-12], which originated from the d orbitals of the heavy metal atoms. In addition, akin to graphene, the conduction and valence-band edges in monolayer MoS<sub>2</sub> are located at the corners (K points) of the 2D hexagonal Brillouin zone, and the two inequivalent valleys constitute a binary index for low energy carriers. Besides, the inversion symmetry in monolayer MoS<sub>2</sub> breaking leads to the valley Hall effect where carriers from different valleys flow to opposite transverse edges when an in-plane electric field is applied[1,5-6]. It is extremely desirable for the spin and valley-based electronic and valley control applications of monolayer MoS<sub>2</sub>[7,9,13].



In this letter, we consider a system where the ferromagnetic ML MoS<sub>2</sub> is placed in the center, both sides being nonferromagnetic. A voltage gate is placed on the top of the ferromagnetic ML MoS<sub>2</sub>. The exchange field can be induced by the magnetic proximity effect by depositing an array of ferromagnetic dysprosium strips.

## 2. Theory and Formula

Now let us explain the formulation. The fermions around the Fermi level in MoS<sub>2</sub> obey a massless relativistic Dirac equation. The Hamiltonian is given by[8]

$$H = \hbar v_F (\tau_z k_x \sigma_x + k_y \sigma_y) + \frac{\Delta}{2} \sigma_z - \lambda \tau_z \frac{\sigma_z - 1}{2} s_z + U + s_z h, \quad (1)$$

U by a voltage gate caused is regarded as in the ferromagnetic region and 0 otherwise, and L is the ferromagnetic region width.  $h$  is the exchange field added in the ferromagnetic region. Where  $\tau_z = \pm 1$  stands for  $K$  and  $K'$  valleys, respectively.  $\sigma_{xyz}$  represents the Pauli matrix in sublattice space.  $s_z = \pm 1$  denotes the spin-up  $\uparrow$  and spin-down  $\downarrow$  components. The Fermi velocity  $v = 5.3 \times 10^5 \text{ m}\cdot\text{s}^{-1}$ ,  $\lambda = 37.5 \text{ meV}$  is the spin splitting induced by the SOC, and  $\Delta = 833 \text{ meV}$  is the band gap.  $h$  is the exchange field added in the ferromagnetic region. According to Eq. (1),  $k'_x$  in the ferromagnetic region is given by

$$k'_x = \{ [E - U - (\tau_z s_z \lambda + s_z h)]^2 - (\Delta - \tau_z s_z \lambda)^2 \}^{\frac{1}{2}} \cdot (\hbar v_F)^{-1}. \quad (2)$$

In the nonferromagnetic regions, the wave vector  $k_x$  can be similarly obtained by substituting  $h=0$ ,  $U=0$  according to Eq. (2). By solving the equation  $H\Psi(x, y) = E\Psi(x, y)$ , and then the spin- and valley-resolved transmission probability can be analytically obtained

$$\begin{aligned} T_{\tau_z s_z} &= \left| \frac{4k_x k'_x E_M E_F \exp(-ik_x L)}{\chi \xi} \right|^2 \\ \xi &= [-E_M^2 k'^2 + 2E_M E_F (k_x k'_x + k_y^2) - E_F^2 k^2] \exp(ik'_x L) \\ \chi &= [E_M^2 k^2 + 2E_M E_F (k_x k'_x - k_y^2) + E_F^2 k^2] \exp(-ik'_x L) \\ E_M &= E - \Delta \quad E_F = E - U - \Delta + s_z h \end{aligned} \quad (3)$$

To evaluate the electron valley- and spin-resolved polarization, we define total tunneling transmission difference  $T_{K(K')}$  and  $T_{\uparrow(\downarrow)}$ , which read

$$T_{K(K')} = \frac{T_{K(K')\uparrow} + T_{K(K')\downarrow}}{2} \quad T_{\uparrow(\downarrow)} = \frac{T_{K\uparrow(\downarrow)} + T_{K'\uparrow(\downarrow)}}{2}.$$

By setting  $k_x = k \cos(\phi)$  and  $k_y = k \sin(\phi)$ , we define the normalized valley and spin resolved conductance

$$G_{\tau s} = \frac{1}{2} \int_{-\frac{\pi}{2}}^{\frac{\pi}{2}} |t_{\tau s}|^2 \cos(\phi) d\phi, \quad (4)$$

then we obtain the valley and spin polarization  $P_v$  and  $P_s$

$$P_v = \frac{(G_{K\uparrow} + G_{K\downarrow}) - (G_{K'\uparrow} + G_{K'\downarrow})}{G_{K\uparrow} + G_{K\downarrow} + G_{K'\uparrow} + G_{K'\downarrow}} \quad P_s = \frac{(G_{K\uparrow} + G_{K'\uparrow}) - (G_{K'\downarrow} + G_{K\downarrow})}{G_{K\uparrow} + G_{K\downarrow} + G_{K'\uparrow} + G_{K'\downarrow}}$$

### 3. Result and discussion

First, to demonstrate the discrepancy of valley and spin transmission, we have calculated the corresponding transmission coefficients of  $T_{K(K')}$  and  $T_{\uparrow(\downarrow)}$ . Figure 1 shows these transmission coefficients versus the incident energy  $E$  with different  $U$ , where figure 1(a) and figure 1(b) correspond to the  $T_{K(K')}$  and  $T_{\uparrow(\downarrow)}$ , respectively. The structure parameters are chosen to be  $L=7\text{nm}$ ,  $\Delta = E_0$ ,  $h = 0.1E_0$  and  $k_y = 0$ . From figure 1(a), when  $U=0.5E_0$ , we can obviously see that the transmission of the  $K'$  electrons and  $K$  electrons in lower energy region is blocked by the barrier. Importantly, the critical energy of  $K'$  electrons is larger than that of the  $K$  electrons. This interesting feature shows that the two valleys have different behavior, leading to valley-polarized transport which is shown in figure 2(a). However, the energy range is extremely narrow. Furthermore, the difference transmission of between  $K$  electrons

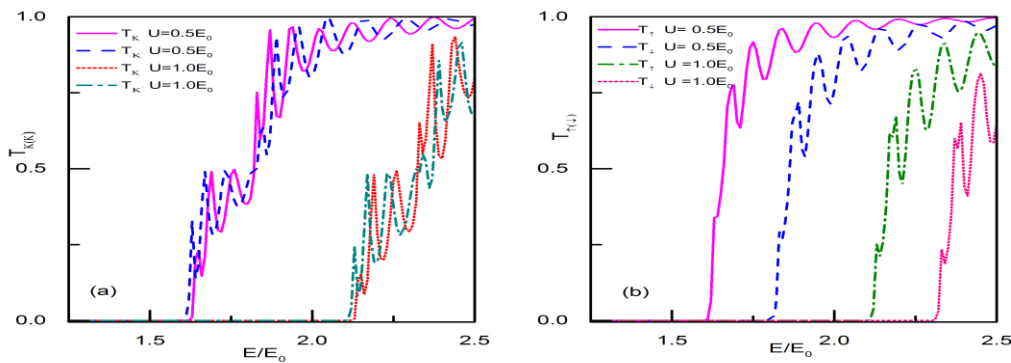


**Figure 1.** (a) Valley transmission and (b) spin transmission as a function of incident energy  $E$  under the manipulation of various  $U$

and  $K'$  electrons in high energy region gradually disappears. For  $U=1.0E_0$ , oscillation of the transmission of  $K$  electrons and  $K'$  electrons are more prominent than  $U=0.5E_0$ . In addition, the increase of  $U$  can expand the range of valley-polarized transport (see the figure 2(a)), owing to the external barrier  $U$  making the conductance band edge shifting upwards. Next, we show the spin resolved transmission and spin-polarized conductance for different  $U$ . We observe that the difference between transmission of spin-up states and transmission of spin-down state are most apparent in figure 1(b). In comparison to the case of the valley resolved transmission, we can see that spin-up state is stronger than that for spin-down one in a wider energy range. Especially, from  $1.55E_0$  to  $1.65E_0$ , spin-down states are absolutely suppressed while spin-up states are filtered out, which results in a fully spin-polarized transport (see the figure 2(b)). Furthermore, it is noted that, for  $U=0.5E_0$  in figure 2(b), a fully spin polarization conductance is obtained in  $1.2E_0$  to  $1.65E_0$  energy range. However, for  $U=1.0E_0$ , it can be seen that spin polarization can be achieved while absent of spin filtering in the same energy range. From  $1.65E_0$  to  $2.2E_0$ , spin-polarized conductance value is up to 1, and this means the spin-polarized conductance can be effectively tuned by the gate voltage.

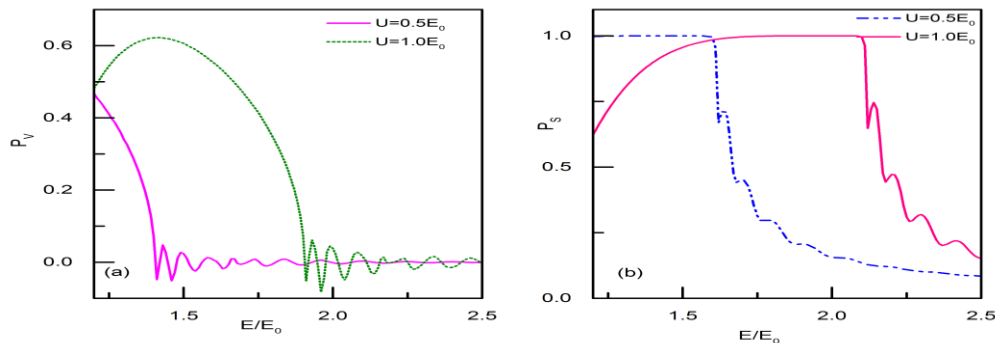


**Figure 2.** (a) Valley-polarized conductance and (b) spin-polarized conductance as a function of incident energy  $E$  under the manipulation of various  $U$ .

#### 4. Conclusion

In summary, we have studied the valley and spin transport in ferromagnetic  $\text{MoS}_2$  junctions. The results showed that a fully spin polarized conductance can be obtained by modulation of the gate voltage. At the same time, valley-polarized transmissions in a small energy area can also be achieved. But the value is only about up to 0.6 by tunneling the gate voltage. These results provide an avenue for the electrical control of valley-and spin-polarized transport in  $\text{MoS}_2$ -based devices.

#### Acknowledgments

This work is supported by NSFC under grants No.11574173 Open Research Fund Program of the State Key Laboratory of Low Dimensional Quantum Physics under grants No.KF201510.

#### References

- [1] Xiao D, Liu G B, Feng W, Xu X and Yao W, *Phys.Rev. Lett.* 2012, **108**, 196802.
- [2] Ellis J K, Lucero M J and Scuseria G E, *Appl. Phys. Lett.* 2011, **99**, 261908.
- [3] Radisavljevic B, Radenovic A, Brivio, J, *Nat. Nanotechnol.* 2011, **6**, 147-150.
- [4] Sarma S D, Adam S, Hwang E H and Rossi E, *Rev. Mod. Phys.* 2011, **83**, 407-470.
- [5] Zhu Z Y, Cheng Y C and Schwingenschlogli U, *Phy. Rev. B* 2011, **84**, 153402.
- [6] Cheiwchanchamnangij T, Lambrecht W R L, *Phys. Rev. B* 2012, **85**, 205302.
- [7] Mak K F, He K, Shan J, Heinz T F, *Nat. Nanotechnol.* 2012, **7**, 494-498.
- [8] Lu H Z, Yao W, Xiao D, Shen S Q, *Phys. Rev.Lett.* 2013, **110**, 016806.
- [9] Cao T, Wang G, Han W, Ye H, Zhu C, Shi, J, Niu Q, Tan P, Wang E, *Nat. Comm.* 2012, **3**, 887.
- [10] Zeng H, Dai J, Yao W, Xiao D and Cui X, *Nat. Nanotechnol.* 2012, **7**, 490-493.
- [11] Yokoyama T, *Phys.Rev.B* 2008, **77**, 073413.
- [12] Haugen H, Huetas-Hernando D, Brataas A, *Phys.Rev.B* 2008, **77**, 115406.
- [13] Yamamoto M, Shimazaki Y, Borzenets I V, Taracha S, *J.Phys. Soc. Jpn.* 2015, **84**, 121006.